CORA Cork Open Research Archive
Cartlann Taighde Oscailte Chorcaí

Title	Correlated electron transport in molecular electronics
Authors	Delaney, Paul A.;Greer, James C.
Publication date	2004
Original Citation	Delaney, P. and Greer, J. C. (2004) 'Correlated electron transport in molecular electronics', Physical Review Letters, 93(3), 036805 (4pp). doi: 10.1103/PhysRevLett.93.036805
Type of publication	Article (peer-reviewed)
Link to publisher's version	https://journals.aps.org/prl/abstract/10.1103/PhysRevLett.93.036805 - 10.1103/PhysRevLett.93.036805
Rights	© 2004, American Physical Society
Download date	2026-11-14 16:32:27
Item downloaded from	https://hdl.handle.net/10468/4654



UCC
University College Cork, Ireland
Coláiste na hOllscoile Corcaigh

Correlated Electron Transport in Molecular Electronics

P. Delaney* and J. C. Greer†

NMRC, University College, Prospect Row, Cork, Ireland‡

(Received 26 November 2003; published 16 July 2004)

Theoretical and experimental values to date for the resistances of single molecules commonly disagree by orders of magnitude. By reformulating the transport problem using boundary conditions suitable for correlated many-electron systems, we approach electron transport across molecules from a new standpoint. Application of our correlated formalism to benzene-dithiol gives current-voltage characteristics close to experimental observations. The method can solve the open system quantum many-body problem accurately, treats spin exactly, and is valid beyond the linear response regime.

DOI: 10.1103/PhysRevLett.93.036805 PACS numbers: 73.63.–b, 71.10.–w, 73.40.Gk

Substantial interest in recent years has been applied to extend the machinery of electronic structure theory, largely developed for study of closed or periodic systems, to open quantum systems. A primary motivation for this effort is the study of electronic transport for nanoscale systems, and specifically the study of molecular electronics [1–4]. Calculations to date use the Landauer-Büttiker formula $\sigma = \mathrm{TG}_0$, to calculate the conductance of a molecule, where $\mathrm{G}_0 = 2e^2/h$ is the conductance quantum [5]. In this formula T is the transmission coefficient of a single-electron wave function $\psi(\mathbf{r})$, so these approaches calculate single-electron wave functions on the molecular junction using an effective single-electron potential. However, the currents flowing through molecular scale systems are consistently predicted to be several orders of magnitude larger than experimentally reported values [1,3,6]. By formulating scattering boundary conditions appropriate to many-body wave functions Ψ, we are able to perform explicitly correlated calculations using the many-body Hamiltonian $\hat{\mathrm{H}}$ which give current magnitudes close to experiment for the prototypical molecular electronics system, benzene-dithiol bonded between two gold contacts.

Central to the study of electronic transport is the concept of two reservoirs locally in equilibrium, but driven out of equilibrium with respect to one another. The corresponding electrochemical potential imbalance drives a current across a device in contact with both reservoirs. Scattering boundary conditions are approximate models of the properties of the electron reservoirs: one reservoir (the left) is associated with the emission of incoming, right moving particles with a fixed equilibrium energy distribution, but capable of absorbing outgoing, left moving particles at any energy; the converse is true for the right reservoir. Implementing scattering boundary conditions for a system of fermions within a single particle approximation is straightforward. Fermi-Dirac statistics $n_F(\epsilon_i \pm eV/2)$, shifted relatively by the bias, are applied to the left and right reservoir incoming wave functions $\psi_i^{L,R}(\mathbf{r})$, thereby inducing a net current flow. In density-functional theory (DFT) computations [7–12] the many-body Coulomb interaction is replaced with an effective one-body exchange-correlation potential, giving single-electron Kohn-Sham wave functions ψ_i; this procedure is formally exact for the ground state total energy of the interacting system. In practice, all exchange-correlation potentials are approximate, and although DFT gives good performance for many properties of closed or periodic systems, it has recently been shown that DFT currents can vary by over an order of magnitude by choosing different approximate potentials [12]. Also, the true exchange-correlation potential is current dependent [13], a fact not explored to date, and the Landauer-Büttiker formula was originally derived for linear response.

In our approach to the electronic transport problem, we avoid these issues by working directly with many-body wave functions $\Psi(\mathbf{r}_1 s_1, \ldots, \mathbf{r}_N s_N)$ and the exact molecular electronic Hamiltonian $\hat{\mathrm{H}}$. By discovering that a form of the single-electron scattering boundary conditions [14] can be generalized to many-body wave functions, we can subsequently apply many-body methods to the electronic structure of open systems. Here we use the configuration interaction (CI) formalism which can give accurate solutions to quantum many-body problems with correct spin eigenfunctions and an equal treatment of ground and excited electronic states; our approach is equally applicable to any other correlated wave function method. In CI we expand the N-electron wave function Ψ in terms of spin-projected Slater determinants

$$\Psi = c_1\Psi_1 + c_2\Psi_2 + \cdots c_L\Psi_L, \tag{1}$$

with expansion coefficients c_μ. We use the exact nonrelativistic electronic Hamiltonian

$$\hat{\mathrm{H}} = -\sum_{n=1,N}\frac{\hbar^2}{2m}\nabla_n^2 + \sum_{n=1,N}\mathrm{U}(\mathbf{r}_n) + \sum_{n<m}\frac{e^2}{|\mathbf{r}_n - \mathbf{r}_m|}, \tag{2}$$

where $\mathrm{U}(\mathbf{r})$ is the attractive potential energy of an electron in the Coulomb field of the atomic nuclei. We then diagonalize the matrix $\mathrm{H}_{\mu\nu}$ of the Hamiltonian in the basis Ψ_μ to find the many-body eigenstates and energies.

 © 2004 The American Physical Society

Working directly with the N-particle wave function Ψ removes a direct physical interpretation of single-electron wave functions $\psi_i(\mathbf{r})$ and eigenvalues ϵ_i from the description of many-electron systems. Therefore, generalization of the conventional single-electron scattering boundary conditions is not possible, and a formulation of the transport problem does not exist for correlated many-electron systems. We resolve this issue by formulating the scattering boundary conditions in terms of the Wigner function $f(q, p)$. For one electron in one dimension, the real function $f(q, p)$ is defined by taking the Wigner transform of the density matrix $\rho(x, x') = \psi^*(x')\psi(x)$, given by

$$f(q, p) = \int_{-\infty}^{+\infty} dr\, \rho(q + r/2, q - r/2)\, \exp(-ipr/\hbar), \tag{3}$$

and it has the advantage of echoing the properties of a classical distribution function (aside for the requirement of strictly positive probabilities) with q and p playing the role of position and momentum, thus giving a phase-space picture of quantum mechanics. For example, expectation values of operator functions $A(\hat{q})$ of position $\hat{q}$ may be expressed as

$$\langle \mathcal{A}(\hat{q}) \rangle = \frac{1}{2\pi\hbar} \int dp\, dq\, \mathcal{A}(q)\, f(q, p) \tag{4}$$

and similarly for functions of momentum $\hat{p}$. The Wigner function also satisfies a quantum Liouville equation with a well-defined classical limit as $\hbar \to 0$ leading to the Boltzmann transport equation. Single-electron scattering boundary conditions can then be applied to a domain $0 \leq x \leq L$ by requiring that $f(0, p > 0)$ and $f(L, p < 0)$ be constrained to their equilibrium values. That is, the momentum distribution of the *incoming electrons* on the left and the right is fixed to values characteristic of the reservoir. The Schrödinger equation is then solved, subject to these boundary conditions, thereby allowing the device to find a steady state by varying the values of the Wigner function in the interior of the device region and at $f(0, p < 0)$ and $f(L, p > 0)$ (the *outgoing electrons*). These boundary conditions were formulated for single-electron wave functions by Frensley [14], and break time-reversal symmetry as is necessary to generate a current-carrying state. In practice, Wigner approaches approximate the density matrix on the infinite contacts by that on the domain $0 \leq x \leq L$ in the integral in Eq. (3). With this approximation, they give similar results to the conventional model of the contacts when applied to one-electron problems; for a resonant tuneling diode, the Wigner and conventional boundary conditions yield current-voltage (IV) curves within a factor of 2–3 [14].

The advantage of the Wigner boundary conditions over the conventional boundary conditions is not improved accuracy but that we can now find a form of the scattering boundary conditions applicable to the many-body problem, and subsequently perform a many-body calculation with no approximate exchange-correlation functional needed and with an exact treatment of spin. We do this by generating the Wigner function $f(\mathbf{q}, \mathbf{p})$ of the correlated wave function Ψ from its one-particle reduced density matrix

$$\rho(\mathbf{r}, \mathbf{r}') = \sum_{s_1} \int d\mathbf{x}_2 \ldots d\mathbf{x}_N \Psi^*(\mathbf{r}' s_1, \mathbf{x}_2, \ldots, \mathbf{x}_N) \times \Psi(\mathbf{r} s_1, \mathbf{x}_2, \ldots, \mathbf{x}_N), \tag{5}$$

where $\mathbf{x}_n = \mathbf{r}_n s_n$. Here, we additionally integrate f over planes perpendicular to the current flow, yielding a one-dimensional Wigner function $f(q, p)$ as above, but our approach does not depend on this simplification. Our example simulation uses the Au_{13}-benzene-dithiolate-Au_{13} contact-molecule-contact system to model the transport region, shown in Fig. 1 (top). Having found the CI ground state of the transport region in the absence of voltage bias, we calculate the equilibrium values of the Wigner function in the left and right contacts $f_0(q_L, p)$ for $p > 0$ and $f_0(q_R, p)$ for $p < 0$; the left contact values are shown in Fig. 1 (middle). Using the one assumption of the Wigner boundary conditions to model the contacts, we can then deduce from the maximum entropy principle [15] at zero temperature the following formulation of the quantum many-body transport problem. The appropriate many-body wave function Ψ for the transport region in the presence of an applied field $\mathcal{E}$ along the molecular axis z minimizes the exact energy $E = \langle \Psi | \hat{\mathbf{H}} + \sum_n e\mathcal{E}\, \hat{\mathbf{z}}_n | \Psi \rangle$ while simultaneously satisfying the open system boundary conditions

$$\langle \Psi | \hat{\mathbf{F}}(q_L, p) | \Psi \rangle = f_0(q_L, p) \quad \text{for } p > 0 \tag{6}$$

and

$$\langle \Psi | \hat{\mathbf{F}}(q_R, p) | \Psi \rangle = f_0(q_R, p) \quad \text{for } p < 0, \tag{7}$$

with normalization constraint $\langle \Psi | \Psi \rangle = 1$ and constraints to enforce current continuity. Here $\hat{\mathbf{F}}(q, p)$ is the Hermitian operator corresponding to the quantity $f(q, p)$, and $\hat{\mathbf{z}}_n$ is the operator for the z coordinate of electron n.

To numerically implement this scheme, we replace the infinite number of constraints implicit in Eqs. (6) and (7) with a finite set of constraints on a grid in momentum space. To solve this nonlinear constrained minimization problem we introduce Lagrange multipliers, deducing their correct values by an iterative optimization technique [16]. In Fig. 1 (bottom) we show the difference between a finite bias and equilibrium Wigner distribution and verify that the minimization procedure respects the boundary constraints. Electron flow results from the difference between these distributions, giving a net electric current to the right. Once the minimizing wave function Ψ has been obtained, we find the current I flowing simply

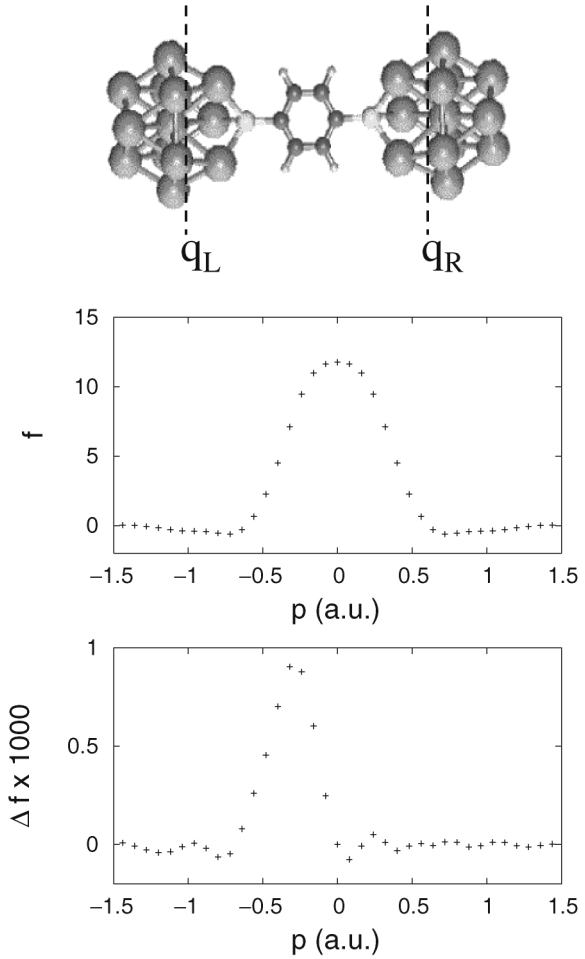


FIG. 1. (top) Geometry of the Au_{13}-benzene-dithiol-Au_{13} junction. (middle) The Wigner momentum distribution function at the left reservoir/device interface at equilibrium ($V = 0$). We use Hartree atomic units for p ($m = 1$, $c \simeq 137$). (bottom) The difference between the finite- and zero-bias Wigner functions at the left contact: note the change in scale. The constraints have fixed the momentum distribution for momenta $p > 0$, while allowing the distribution at $p < 0$ to vary.

by integrating the probability current density $\mathbf{J}(\mathbf{r})$ over planes perpendicular to the molecular axis.

For our prototype transport calculation, we begin with a fully relaxed structure (no strain at zero current) consisting of the benzene-dithiolate molecule bonded between the (111) faces of two gold clusters in C_{2v} symmetry [17]; see Fig. 1 (top). A set of many-body expansion functions for this structure was selected using the Monte Carlo configuration interaction method [18,19]. Exact spin coupling is applied and the zero-bias total system eigenfunction Ψ_0 is a singlet for the ground state. In Fig. 2, we present our computed IV characteristics for the benzene-dithiol system. The IV curve has been generated by increasing the applied field $\mathcal{E}$ in steps and finding the energy-minimizing wave function at each field. The voltage is then calculated by integrating the

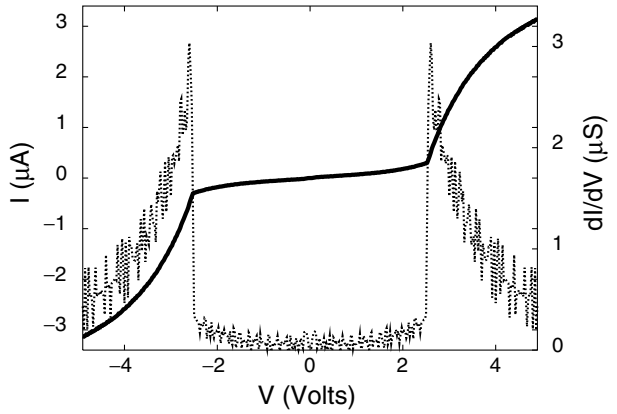


FIG. 2. Calculated current-voltage characteristics for benzene-dithiolate bonded to the (111) faces of two gold clusters; also shown is the differential conductance dI/dV.

external electric field between the two reservoir/device interface planes where the Wigner constraints are applied.

We find two distinct regions in the resulting IV characteristics, with an abrupt transition between the two near 2.5 V. We can trace the origins of this transition by examining the polarization behavior of the isolated Au_{13}-benzene-dithiolate-Au_{13} system under application of an external field. By removing the Wigner constraints we decouple the transport region from the gold wires; in Fig. 3 we show the energies of the first five eigenstates as the applied field is increased. The isolated ground and first excited state respond slowly to the applied field, due to the large energy denominators occurring in second order perturbation theory, while the three closely spaced states $|2A_1\rangle$, $|3A_1\rangle$, and $|2B_2\rangle$ couple strongly, giving a state

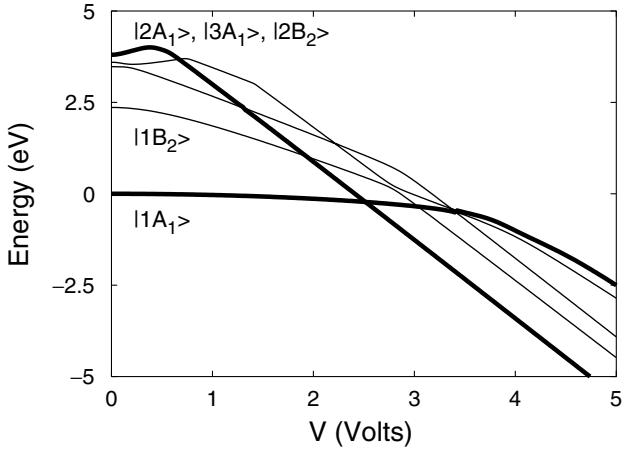


FIG. 3. Energies of the lowest five CI eigenstates as a function of applied field, for the isolated (no Wigner constraints) Au_{13}-benzene-dithiolate-Au_{13} cluster. The energy levels are labeled by the irreducible representation of C_{2v} by which they transform at zero field, and by energy ordering within this irrep. The field mixes the states of A_1 and B_2 symmetry together.

which polarizes rapidly with the field and crosses the ground state at 2.5 V.

Electron correlation refers to physics beyond that describable by a single Slater determinant. The eigenvalues of the reduced density matrix $\rho(\mathbf{r}, \mathbf{r}')$ are the natural orbital occupancies n_i; a necessary condition for Ψ to originate from some single determinant is that $n_i = 2$ for $N/2$ occupied orbitals and $n_i = 0$ for all others. The CI wave function at $V = 0$ has a typical pattern of occupancies slightly changed from that of a single determinant, and this remains the same up to the transition. Above the transition, however, we see a significant number of orbitals whose occupancies differ from 2 or 0. Taken together with the excited state influence on the transition voltage, we see that electron correlation is essential for an accurate description of molecular electronic transport.

We note here that the current magnitude below resonance is in good agreement with experiment [1], particularly when compared to other theoretical predictions, and the qualitative behavior of the IV characteristic is consistent with other recent findings of molecular scale transport, with nonresonant tunnel regimes followed by a rapid increase in current magnitude [6]. Our calculations indicate an onset resistance of 18 MΩ and a resonant tunnel resistance of several MΩ, close to the corresponding experimental values of ≈22 and ≈13 MΩ estimated by Reed *et al.* Previous *ab initio* DFT calculations typically find currents in the range of 20 000 to 60 000 nAmps at 2 V [8,11], whereas we find a current of 179 nAmps which compares favorably with the experimental measurement of ≈60 nAmps [1]. Our calculation has two distinct sources of error: the finite CI expansion used, and the use of boundary conditions (in our case, the Wigner boundary conditions) to model the reservoirs. From test calculations, we estimate an overall factor of 3 due to these approximations, so the order of magnitude of the current is quite stable. We have also investigated the effect of geometry distortion: stretching the sulpur to gold contact distance by 0.25 Å reduces the current by typically 30% below the transition.

In conclusion, we have presented an approach to electronic transport that represents a radical departure from either scattering theory or Green's function methods. The formalism is conceptually simple, and is made possible by a generalization of the scattering boundary conditions to many-body calculations. Our method yields many-body wave functions which are exact eigenstates of spin and so can also be used for studying spin-dependent transport and Kondo effect physics. For benzene-dithiolate, we calculate electronic currents orders of magnitude lower than other theoretical predictions, but of the correct order of magnitude with respect to the experimental measurements, the first such result to our knowledge. We hypothesize that as DFT exchange correlation functionals have been developed to reproduce an integrated quantity (the energy), they must be modified for accurate treatment of transport by determining exchange-correlation potentials that are locally accurate. We note that for accurate molecular electronics simulation, it appears that a highly correlated treatment of the electronic structure is needed.

This work was supported by the European Union's Future & Emerging Technology programme through the Nanotcad project and by Science Foundation Ireland.

*Email address: paul.delaney@nmrc.ie
†Email address: jim.greer@nmrc.ie
‡Web address: http://www.nmrc.ie/research/computational-modelling-group/index.html

[1] M. A. Reed *et al.*, Science **278**, 252 (1997).
[2] C. Joachim, J. K. Gimzewski, and A. Aviram, Nature (London) **408**, 541 (2000).
[3] A. Nitzan and M. A. Ratner, Science **300**, 1384 (2003).
[4] M. H. Hettler, W. Wenzel, M. R. Wegewijs, and H. Schoeller, Phys. Rev. Lett. **90**, 076805 (2003).
[5] R. Landauer, Philos. Mag. **21**, 863 (1970); M. Büttiker, Y. Imry, R. Landauer, and S. Pinhas, Phys. Rev. B **31**, 6207 (1985).
[6] J. O. Lee *et al.*, Nano Lett. **3**, 113 (2003).
[7] E. G. Emberly and G. Kirczenow, Phys. Rev. B **58**, 10 911 (1998).
[8] M. Di Ventra, S. T. Pantelides, and N. D. Lang, Phys. Rev. Lett. **84**, 979 (2000).
[9] P. A. Derosa and J. M. Seminario, J. Phys. Chem. B **105**, 471 (2001).
[10] P. S. Damle, A.W. Ghosh, and S. Datta, Phys. Rev. B **64**, 201403 (2001).
[11] K. Stokbro *et al.*, Comput. Mater. Sci. **27**, 151 (2003).
[12] P. S. Krstić *et al.*, Comput. Mater. Sci. **28**, 321 (2003).
[13] G. Vignale and M. Rasolt, Phys. Rev. Lett. **59**, 2360 (1987).
[14] W. R. Frensley, Phys. Rev. Lett. **57**, 2853 (1986); **60**, 1589 (1988); Rev. Mod. Phys. **62**, 745 (1990).
[15] E. T. Jaynes, Phys. Rev. **106**, 620 (1957).
[16] J. Nocedal and S. J. Wright, *Numerical Optimization* (Springer Verlag, New York, 1999).
[17] J. A. Larsson, M. Nolan, and J. C. Greer, J. Phys. Chem. B **106**, 5931 (2002).
[18] J. C. Greer, J. Comput. Phys. **146**, 181 (1998).
[19] Effective core potentials were applied to all gold atoms (78 core electrons) and to the bonding sulfur atoms (10 core electrons). Atomic basis sets: Au, sp on 20 atoms, spd on the 6 bonding gold atoms; S, $2s2p$; C $4s2p1d$; H $2s$. Many-body basis set: the three lowest zero-field A_1 and B_2 CI eigenstates were determined, using an acceptance criteria $c_{\min} = 10^{-2}$. We concatenated these six configuration sets to form the transport basis set.